Technical Note

Elimination of high concentration hydrogen sulfide and biogas purification by chemical–biological process

Kuo-Ling Ho [a,1,2], Wei-Chih Lin [a,1], Ying-Chien Chung [b], Yu-Pei Chen [b], Ching-Ping Tseng [a,*]

[a] Department of Biological Science and Technology, National Chiao Tung University, Hsinchu 300, Taiwan
[b] Department of Biological Science and Technology, China University of Science and Technology, Taipei 115, Taiwan

HIGHLIGHTS

- We constructed the chemical–biological H_2S removal system in lab and pilot scale.
- The pilot system had operated consecutive 311 d for livestock biogas purification.
- Stable cell density and iron ratio contributed to high H_2S removal performance.
- The change of microbial populations was analyzed in pilot scale study.
- This process is feasible for high concentration H_2S elimination from biogas.

ARTICLE INFO

ABSTRACT

A chemical–biological process was performed to remove a high concentration of H_2S in biogas. The high iron concentration tolerance ($20\ g\ L^{-1}$) of Acidithiobacillus ferrooxidans CP9 provided sufficient ferric iron level for stable and efficient H_2S elimination. A laboratory-scale apparatus was setup for a 45 d operation to analyze the optimal conditions. The results reveal that the H_2S removal efficiency reached 98% for 1500 ppm H_2S. The optimal ferric iron concentration was kept between 9 and $11\ g\ L^{-1}$ with a cell density of $10^8\ CFU\ g^{-1}$ granular activated carbon and a loading of $15\ g\ S\ m^{-3}\ h^{-1}$. In pilot-scale studies for biogas purification, the average inlet H_2S concentration was 1645 ppm with a removal efficiency of up to 97% for a 311 d operation and an inlet loading $40.8\ g\ S\ m^{-3}\ h^{-1}$. When 0.1% glucose was added, the cell density increased twofold under the loading of $65.1\ g\ S\ m^{-3}\ h^{-1}$ with an H_2S removal efficiency still above 96%. The analysis results of the distribution of microorganisms in the biological reactor by DGGE show that microorganism populations of 96.7% and 62.7% were identical to the original strain at day 200 and day 311, respectively. These results clearly demonstrate that ferric iron reduction by H_2S and ferrous iron oxidation by A. ferrooxidans CP9 are feasible processes for the removal of H_2S from biogas.

1. Introduction

Corrosive H_2S associated with biogas is produced via the anaerobic digestion of biodegradable materials, which hinders the utilization of biogas. Several gas purification processes have been applied to eliminate H_2S, such as chemical scrubbing, physical adsorption (Belmabkhout et al., 2009), electrochemical treatment (Chang and Tseng, 1996), and biofiltration (Duan et al., 2007; Ho et al., 2008). Although physical and chemical treatments are rapid and efficient, their high cost and production of secondary pollutants are unfavorable.

Biological processes that directly metabolize H_2S into sulfate in an efficient and inexpensive way have been reported. However, the drop in pH caused by sulfate accumulation has negative effects (Lee et al., 2006; González-Sánchez et al., 2008; Jiang et al., 2009). Therefore, studies on biological processes have focused on removing low H_2S concentrations (10–50 ppm) to prevent rapid pH drop (Gabriel, 2003; Kim et al., 2008; Goncalves and Govind, 2009; Ryu et al., 2009; Ramírez et al., 2011).

Other studies that combined chemical and biological processes for both H_2S elimination and ferric iron regeneration by Acidithiobacillus ferrooxidans have been reported (Giro et al., 2006; Alemzadeh et al., 2009). These processes are based on two reactions as follows: the inlet H_2S is first oxidized with a ferric iron solution and yields elemental sulfur, and the reduced ferrous iron is then reoxidized by A. ferrooxidans in the biological process.

Separate studies that focused on chemical absorption (Asai et al., 1990; Ebrahimi et al., 2003) and biological oxidation (Mousavi et al., 2008; Alemzadeh et al., 2009) were proposed. For instance, when the inlet H_2S concentration is lower than 300 ppm, the rate-limiting step for the chemical absorption process is the mass-transfer limitation, as revealed by model validation (Chung et al., 2003). When the system has a high inlet H_2S concentration (e.g., above 1500 ppm), the H_2S removal efficiency is significantly maintained via long GRT (gas retention time) and stable ferric iron concentration in the chemical reactor (Chung et al., 2006). In the biological reaction, Mesa et al. (2004) investigated the continuous oxidation efficiency of ferrous iron by using immobilized A. ferrooxidans. However, studies that focused on the combined and continuous operation are limited.

In the present study, the chemical absorption reactor and the biological oxidation reactor with immobilized A. ferrooxidans CP9 were connected and then examined in both laboratory and pilot scales to evaluate the performance of H_2S elimination. In the laboratory-scale study, optimal operating parameters such as GRT, temperature, and H_2S inlet loading were examined. In the pilot-scale study, the biogas with an average H_2S concentration of 1645 ppm was introduced into the chemical–biological system. The long-term performance was examined, and the results demonstrate that the chemical–biological process effectively removed H_2S from the biogas.

2. Material and methods

2.1. Microorganism and cultivation

A. ferrooxidans CP9 was isolated from an acid mine drainage, and then identified by the 16S rRNA gene (GenBank accession number EF605251). This strain was grown in the M16 broth medium (Kim et al., 2002). A solid KBU medium was prepared for cell number counting of A. ferrooxidans CP9 (Khalid et al., 1993).

In the immobilization process, granular activated carbon (GAC) with a diameter of 4.5 mm and a surface area of $1250 \, m^2 \, g^{-1}$ was used (China Activated Carbon Industries, Taiwan) to immobilize the A. ferrooxidans CP9 in the bioreactor. The details of the procedure were described in a previous report (Chung et al., 2006). The cell-laden GAC was transferred to the bioreactor when the cell density reached $10^8 \, CFU \, g^{-1}$ GAC.

2.2. Combined chemical–biological reactor for H_2S elimination

A scheme of the combined chemical–biological system on a laboratory scale is shown in Fig. 1. The 1% H_2S gas, which was supplied from a gas cylinder, was initially diluted with compressed air, and then pumped into the bottom of the chemical reactor. The glass chemical reactor (12 cm id × 50 cm H) with a height of 40 cm was filled with the M16 medium, which contained glass beads (id: 6 mm). A perforated sieve plate at the bottom of the reactor allowed the H_2S gas to flow in. The bioreactor (12 cm id × 50 cm H) with a height of 40 cm was packed with GAC to immobilize A. ferrooxidans CP9 in the M16 medium. The bioreactor was fitted with a thermostatic jacket to control the temperature. A funnel-shaped sulfur separation tank was set between the chemical and biological reactors to collect the elemental sulfur. The circulation of the medium between each column was driven by a peristaltic pump at specific circulating rates.

The composition of the pilot scale chemical–biological reactor was similar to that shown in Fig. 1, except the height is 150 cm. The biogas produced from the anaerobic wastewater treatment system was pumped into the chemical reactor at specific flow rates. The maintenance of liquid level and glucose concentration in this system was checked weekly during the operation.

2.3. DGGE and phylogenetic analysis

The PCR primers of 968f GC and 1401r were used to amplify the segment of the eubacterial 16S rDNA (Brosius et al., 1981). The process of manipulating the extracted genomic DNA and the amplified PCR is shown in a previous study (Ho et al., 2008). The samples were run on 8% acrylamide gel with a denaturant gradient between 45% and 60% by using a Bio-Rad DGGE apparatus. The electrophoresis procedure was run, stained, and rinsed, as described in a previous report (Torsvik et al., 2000). The interesting fragments were excised from the DGGE gels for DNA amplification and sequencing. Phylogenetic trees were constructed from the evolutionary distance by using the Tree View software.

2.4. Analytical methods

H_2S concentrations were measured using gas detector tubes (Kitagawa). Ferrous, ferric, and total iron concentrations were determined using a previously described method (Chung et al., 2006). For cell density analyses, 0.5 g of GAC was collected from the bioreactor and vortexed with 5 mL of sterile water for 5 min, and sprayed on the solid KBU medium. The dark-brown colony in the medium was indicated as A. ferrooxidans CP9 after 7–14 d of cultivation.

3. Results and discussion

3.1. Effects of inlet H_2S concentration on removal efficiency and Fe^{2+}/Fe^{3+} ratio in the laboratory scale

The influence of H_2S concentration on chemical absorption behavior was examined in the laboratory-scale combined reactor. Fig. 2a shows the effect of inlet H_2S concentration on the efficiency of the system during the 45 d operation with a GRT of 8 min. The results indicate that the removal efficiency increased with decreasing inlet H_2S concentration during the first 15 d. A removal efficiency of 98% was achieved when the inlet H_2S concentration was less than 1500 ppm. Fig. 2b and c show the variation in Fe^{2+}/Fe^{3+} ratio and pH during the 45 d operation. The ferric iron consumption rate and the ferrous iron accumulation rate were proportional to the inlet H_2S concentration. In the high loading stage
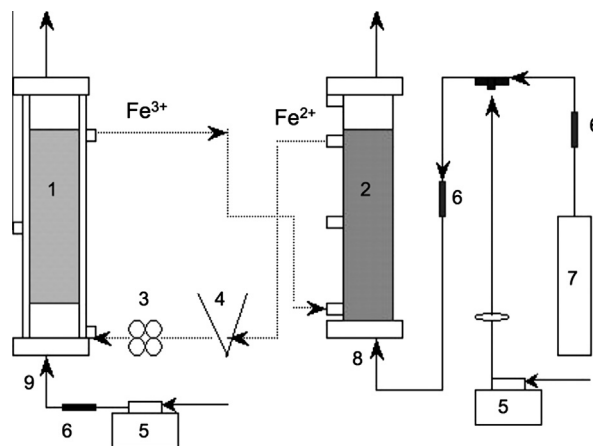

Fig. 1. A schematic of the laboratory scale combined chemical–biological reactor for H_2S treatment: (1) biological column, (2) chemical column, (3) liquid peristaltic pump, (4) sulfur storage tank, (5) air pump, (6) gas flow meter, (7) H_2S gas cylinder, (8) inlet of H_2S, and (9) inlet of air.

(2000 ppm), the H₂S removal efficiency decreased when the ferric iron decreased to 6 g L⁻¹ in the chemical reactor. On the other hand, when H₂S was fed at 1000 ppm, the ferrous and ferric iron concentrations remained stable between 9 and 11 g L⁻¹ (Fe^{2+}/Fe^{3+} = 1 ± 0.2) in both reactors and then reached a removal efficiency of over 99%. Therefore, when GRT was kept at 8 min, the system maintained the Fe^{2+}/Fe^{3+} ratio and achieved high removal efficiency when the inlet H₂S concentration was between 1000 and 1500 ppm. Giro et al. (2006) treated a gas with a high H₂S concentration (20000 ppm) by using a combined chemical–biological system; however, they used a lower H₂S loading (10.9 g S m⁻³ h⁻¹) and a shorter operation time (600 min) compared with this study.

The effect of inlet loading change on biological behavior was also examined. The variations in pH (pH 1.7–1.9) and cell density (6 × 10⁷ to 7 × 10⁷ CFU g⁻¹ GAC) were stable despite the H₂S inlet concentrations. After the shock loading test (from day 10 to 15), the system showed a remarkable ability for recovery. Although the ferrous iron concentration was continuously kept above 14 g L⁻¹ during the shock loading test, cell growth was not negatively affected.

3.2. Effects of GRT on H₂S removal efficiency and Fe²⁺/Fe³⁺ concentration in the laboratory scale

In the 90 d continuous experiment, the GRT was gradually decreased to increase the H₂S loading value. Fig. 3 shows the effect of GRT on the H₂S removal efficiency and Fe^{2+}/Fe^{3+} concentration at an inlet H₂S concentration of 1000 ppm. The results indicate that the H₂S removal efficiency dropped to 82% when the GRT was 4 min (Fig. 3a), and further dropped to 15% when the GRT was 1 min. The ferric iron concentration in the chemical reactor decreased with decreasing GRT (Fig. 3b) and caused a drop in the

removal efficiency. The ferric iron regeneration rate in the biological reactor was insufficient to support H₂S oxidization in the chemical reactor during day 65–90 (Fig. 3c). In the first 30 d, the H₂S removal efficiency reached 100% when the ferric iron concentration was about 10 g L⁻¹, but continuously dropped to less than 90% when the ferric iron concentration was less than 6 g L⁻¹. This result is consistent with those of Mesa et al. (2004), who concluded that the maximum H₂S absorption efficiency is reached when the ferric iron concentration is between 10 and 13 g L⁻¹, but remarkably decreased in the lower concentration region.

In this laboratory-scale combined system, an H₂S loading over 40 g S m⁻³ h⁻¹ decreased the H₂S removal efficiency to below 90% because of ferric iron consumption. A previous report (Pagella and De Faveri, 2000) applied a loading of 66 g S m⁻³ h⁻¹ in a combined system. However, the inlet H₂S concentration was low (100 ppm), and the removal efficiency dropped to 30% after the 12 d operation due to the ferric iron concentration continuously dropped. This result was attributed to the insufficient biological oxidative ability of the bioreactor and the failure to remove sulfur precipitates from the chemical absorber; hence, both factors reduced the mass transfer efficiency of the liquid–H₂S interface (Pagella and De Faveri, 2000).
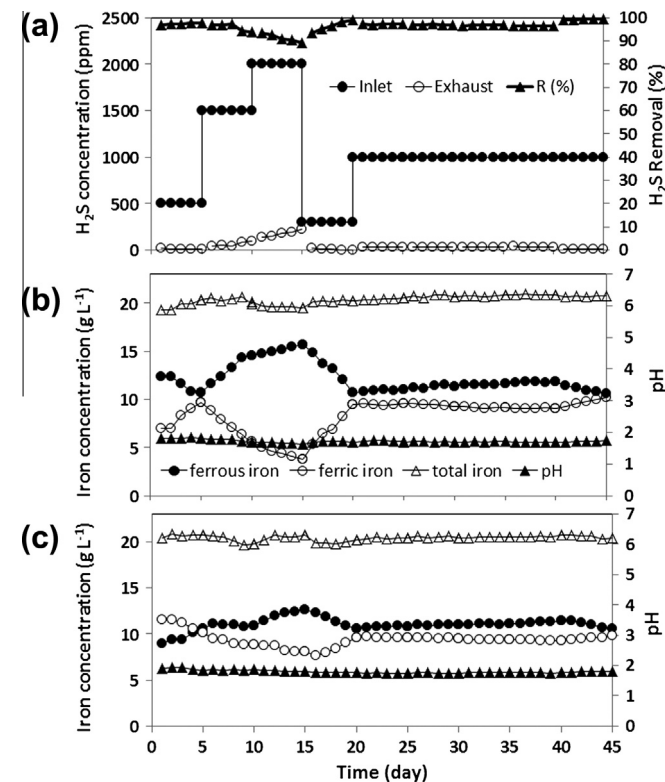

Fig. 2. Laboratory scale H₂S elimination in various inlet concentrations of the 45 d operation. (a) H₂S inlet/outlet concentration and removal efficiency. The iron concentration plot in (b) chemical reactor and (c) bioreactor.
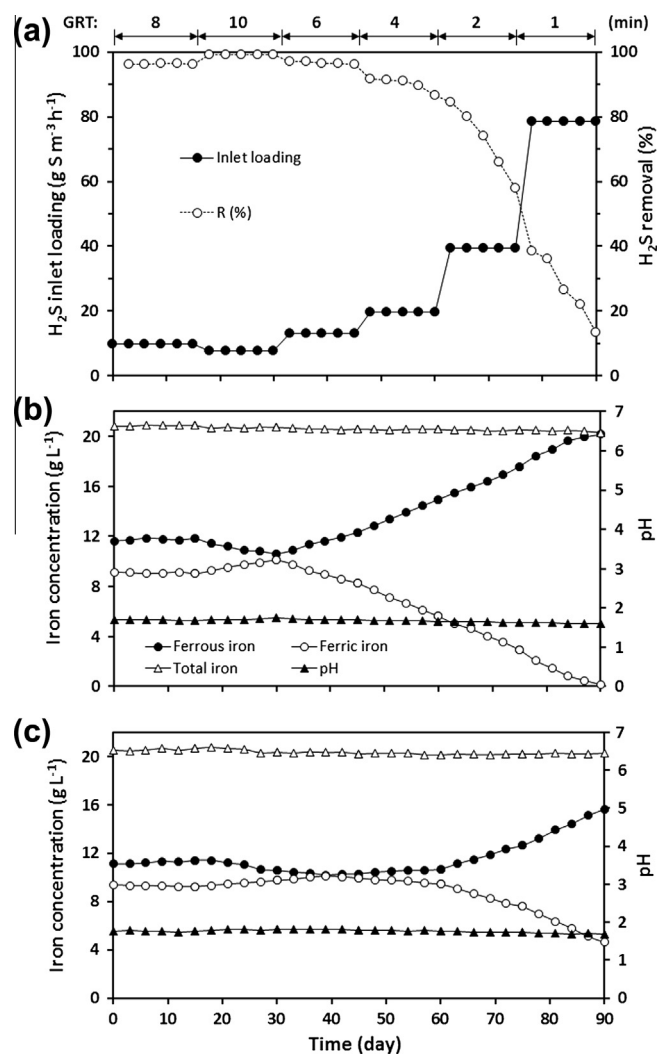

Fig. 3. Laboratory scale H₂S elimination in various GRT of the 90 d operation. (a) Loading and removal efficiency plot. The iron concentration profile in (b) chemical reactor and (c) bioreactor.

3.3. Effect of temperature on system performance in the laboratory scale

Gomez et al. (2000) found that the ferrous iron oxidation efficiency of A. ferrooxidans dramatically decreases when the temperature was increased from 30 to 40 °C. In addition, the ferrous iron oxidation efficiency of A. ferrooxidans was weak at 40 °C in the bioreactor (Chung et al., 2003). We conducted a 30 d test to analyze further the effects of temperature on the performance of the combined system. The six stages were 35, 26, 18, 26, 42, and 26 °C, and each stage lasted for five days. The experimental conditions were kept at 8 min GRT, 1,500 ppm H_2S concentration (15 g S m^{-3} h^{-1} loading), and 3 L min^{-1} medium circulation rate. The results show that the removal efficiency reached 99% in all stages except at 42 °C, which was slightly lower at 97%. The high efficiency was likely due to the buffering ability of chemical adsorption. Although the ferric iron concentration declined at 42 °C, it remained greater than 8 g L^{-1} and was enough to oxidize H_2S efficiently. Nevertheless, the number of A. ferrooxidans CP9 cells decreased to 1/2 and 1/8 at 18 and 42 °C, respectively, compared with that at 35 °C. Apparently, the relatively low cell density in the bioreactor at 42 °C slowed the ferrous iron oxidation efficiency and slightly decreased the H_2S removal efficiency. The oxidation efficiencies of 20.1, 33.4, 29.2, and 12.6 mg L^{-1} h^{-1} were determined at conditions of 18, 26, 35, and 42 °C, respectively. The different oxidation efficiencies explain the minor variations in H_2S removal efficiency. Moreover, the results show that the combined chemical–biological system could be applied within a broad temperature range.

3.4. Effect of loading and carbon source on biogas purification in the pilot-scale study

The biogas composition (%) in this study was 61 ± 9 CH_4, 26 ± 4 CO_2, 4 ± 1 O_2, and 1645 ± 345 ppm H_2S in average during the 311 d continuous operation. The GRT was kept at 3 min in the first 150 d and then reduced to 2 min during day 151–311. The liquid circulation rate was maintained at 2 mL min^{-1}, and the initial Fe^{2+}/Fe^{3+} concentrations were both at 10 g L^{-1}. Fig. 4a shows the H_2S removal efficiency at different H_2S concentrations ranging from 890 to 2250 ppm in the inlet biogas. The average H_2S removal efficiencies for the stages without (day 1–90) and with (day 91–311) glucose were both about 98%.

The GRT decreased to 2 min during day 151–311, although the increased H_2S loading led to the accumulation of ferrous iron, the ferric iron concentration remained above 6 g L^{-1}, and the average H_2S removal efficiency was sustained at 97%. In previous studies, biofilters with shorter GRTs (1.6–30 s) were applied in the field to treat waste gases containing H_2S (Gabriel, 2003; Duan et al., 2005, 2007). However, the inlet H_2S concentrations were operated below 100 ppm in these studies.

In this pilot-scale operation, the ferric iron concentration in the chemical reactor was initially kept stable in the first 50 d and then slightly decreased from 10 to 8.4 g L^{-1} during day 50–90. However, it recovered to 9.2 g L^{-1} in the next 60 d after the addition of 0.1% glucose (Fig. 4b and c). The average cell density with glucose was 8 × 10^8 CFU g^{-1} GAC, which was twofold higher than that without glucose. Therefore, the elevated ferric iron concentration after the addition of 0.1% glucose (day 50–90) was attributed to the increase in cell density in this operation.

During day 151–311 of high H_2S loading (65.1 g S m^{-3} h^{-1} on the average), the formation rate of ferric iron in the bioreactor was not fast enough compared with the consumption rate in the chemical process. However, the cell density increased to 9 × 10^8 CFU g^{-1} GAC with 0.1% glucose and then neutralized the high H_2S loading effect. Therefore, the addition of glucose caused the variation in ferric iron concentration in the chemical reactor, which
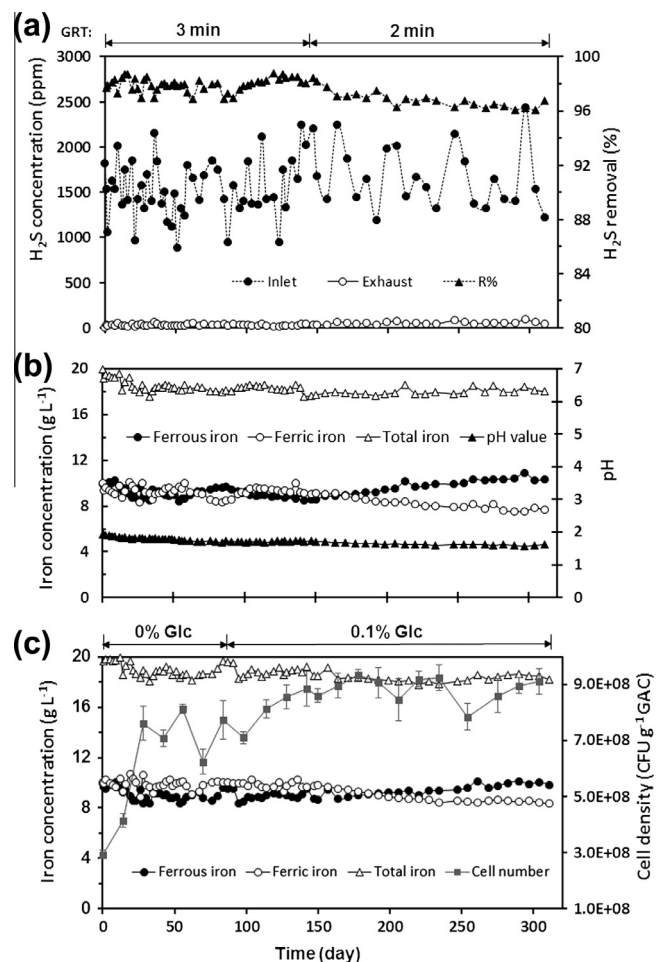

Fig. 4. Biogas purification in the pilot scale of 311 d operation. (a) H_2S inlet/outlet concentration and removal efficiency. (b) The iron concentration plot in chemical reactor. (c) The iron concentration and cell density plot in bioreactor.

merely decreased from 9.2 to 7.7 g L^{-1}. This result was in agreement with a previous laboratory-scale study, where the addition of glucose improved the iron oxidation ability of A. ferrooxidans (Chung et al., 2006).

3.5. Analysis of the microorganism community during pilot-scale operation

PCR-DGGE was used to determine the variations in bacterial communities. Fig. 5 shows the profile of the DGGE bands during the 311 d operation. The complexity of the DGGE bands increased with increasing operating time. These bands show that exotic bacterial populations appeared after glucose was added. However, band B (inoculated A. ferrooxidans CP9) was a consistently dominant population in the bacterial consortium throughout the operation time. The intensity of band B on day 90 was 100%, which indicates that only A. ferrooxidans was detected in this system. Three minor microbes that comprise bands C (0.9%), J (0.2%), and K (2.2%) appeared on day 200, but the intensity of band B remained as high as 96.7%.

On the day 311, ten discernible bands were observed, namely, bands A (4.3%), B (62.7%), C (5.4%), D (1.7%), E (7.3%), F (2.4%), G (6.8%), H (6.7%), I (1.7%), and J (1%). Band B was the most intense and predominant band, which was identified as A. ferrooxidans (99%). Bands C and H belonged to phylum proteobacteria. Their close relatives shared close similarities to Acidithiobacillus sp.
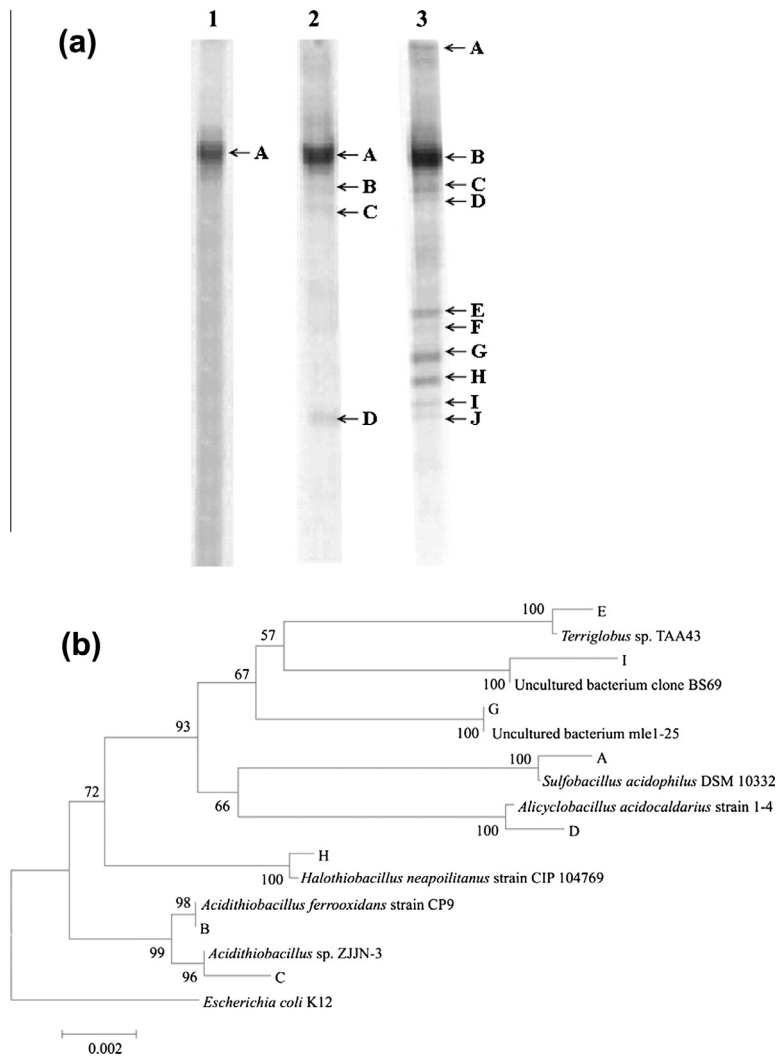
Fig. 5. Analysis of the microorganism community during pilot scale operation. (a) DGGE analysis for day 90, 200, and 311. (b) Plot of the phylogenetic trees.

ZJJN-3 (98%) and *Halothiobacillus neapolitanus* strain CIP 104769 (99%). Three bands (E, G, and I) were clustered to the phylum *Acidobacteria*, namely, *Terriglobus* sp. TAA 43 (97%), uncultured bacterium mle1-25 (98%), and uncultured bacterium clone BS69 (96%). Two bands (A and D) were grouped to the phylum *Firmicutes*, namely, *Sulfobacillus acidophilus* strain GG6/1 (99%) and *Alicyclobacillus acidocaldarius* strains 1–4 (98%). Bands F and J were too weak and could not be identified.

According to these results, all sequences were identified as aerobic and acidophilic bacteria with an optimal growth pH ranging from 2 to 4. Most microbes were autotrophic, except for *S. acidophilus* (band A), *A. acidocaldarius* (band D), and *Terriglobus* sp. (band E), which were mixotrophic, heterotrophic, and oligotrophic, respectively (Eichorst et al., 2007). This result suggests that the addition of glucose increased the complexity of the microbial communities. Johnson et al. (2005) showed that *S. acidophilus* (band A), which was similar to the inoculated *A. ferrooxidans*, possesses reducing power from oxidizing ferrous iron or sulfur. Besides, the *H. neapolitanus* (band H) was designated as a sulfur-oxidizing bacterium (García-de-la-Fuente et al., 2011). Minor elemental sulfur formed by the H_2S oxidation reaction in the chemical reactor was expected to migrate to the bioreactor through medium circulation and could be an energy source to some exclusively sulfide-oxidizing bacteria.

Although the extra carbon source gave rise to the appearance of exotic microbes in the system, it also increased the cell density of the inoculated strain by twofold compared with the cell density in the earlier 90 d of the operation. On day 311, *A. ferrooxidans* was still dominant at 62.7%, and the H_2S removal efficiency was maintained at 96%. This result showed that the ferrous oxidation ability of this system did not decrease with increasing microbial complexity.

4. Conclusions

We demonstrated that the chemical–biological process immobilized with iron-tolerant *A. ferrooxidans* CP9 maintained the balance of the Fe^{2+}/Fe^{3+} ratio and reached an H_2S removal efficiency of 98%. In the pilot-scale operations, the addition of glucose improved the biogas purification efficiency by increasing the cell density and ferrous oxidation efficiency. The H_2S loading reached 65.1 g S m^{-3} h^{-1} (3.3-fold higher than the laboratory-scale condition) with a removal efficiency of 96%. In addition, the factors of high tolerance for iron ions at 20 g L^{-1} and the rapid ferrous iron oxidation ability of *A. ferrooxidans* CP9 were important in maintaining the balance of Fe^{2+}/Fe^{3+} concentrations. Although the exotic microbes appeared during the 311 d operation, the *A. ferrooxidans* CP9 cell density remained more than 10^8 CFU g^{-1} GAC and offered a stable ferrous iron oxidation ability. These results clearly demonstrate that the chemical–biological process is a feasible method for eliminating high H_2S concentration from biogas.

Acknowledgements

References

Alemzadeh, I., Kahrizi, E., Vossoughi, M., 2009. Bio-oxidation of ferrous ions by *Acidithioobacillus ferrooxidans* in a monolithic bioreactor. J. Chem. Technol. Biotechnol. 84, 504–510.

Asai, S., Konishi, Y., Yabu, T., 1990. Kinetics of absorption of hydrogen sulfide into aqueous ferric sulfate solutions. AIChE J. 36, 1331–1338.

Belmabkhout, Y., De Weireld, G., Sayari, A., 2009. Amine-bearing mesoporous silica for CO_2 and H_2S removal from natural gas and biogas. Langmuir 25, 13275–13278.

Brosius, J., Dull, T.J., Sleeter, D.D., Noller, H.F., 1981. Gene organization and primary structure of a ribosomal RNA operon from *Escherichia coli*. J. Mol. Biol. 148, 107–127.

Chang, M., Tseng, T., 1996. Gas-phase removal of H_2S and NH_3 with dielectric barrier discharges. J. Environ. Eng. 122, 41–46.

Chung, Y.C., Ho, K.L., Tseng, C.P., 2003. Hydrogen sulfide gas treatment by a chemical–biological process: chemical absorption and biological oxidation steps. J. Environ. Sci. Health, Part B 38, 663–679.

Chung, Y.C., Ho, K.L., Tseng, C.P., 2006. Treatment of high H_2S concentrations by chemical absorption and biological oxidation process. Environ. Eng. Sci. 23, 942–953.

Duan, H., Koe, L.C.C., Yan, R., 2005. Treatment of H_2S using a horizontal biotrickling filter based on biological activated carbon: reactor setup and performance evaluation. Appl. Microbiol. Biotechnol. 67, 143–149.

Duan, H., Yan, R., Koe, L.C.C., Wang, X., 2007. Combined effect of adsorption and biodegradation of biological activated carbon on H_2S biotrickling filtration. Chemosphere 66, 1684–1691.

Ebrahimi, S., Kleerebezem, R., van Loosdrecht, M., Heijnen, J., 2003. Kinetics of the reactive absorption of hydrogen sulfide into aqueous ferric sulfate solutions. Chem. Eng. Sci. 58, 417–427.

Eichorst, S.A., Breznak, J.A., Schmidt, T.M., 2007. Isolation and characterization of soil bacteria that define *Terriglobus* gen. nov., in the phylum *Acidobacteria*. Appl. Environ. Microbiol. 73, 2708–2717.

Gabriel, D., 2003. Retrofitting existing chemical scrubbers to biotrickling filters for H_2S emission control. Proc. Natl. Acad. Sci. 100, 6308–6312.

García-de-la-Fuente, R., Cuesta, G., Sanchís-Jiménez, E., Botella, S., Abad, M., Fornes, F., 2011. Bacteria involved in sulfur amendment oxidation and acidification processes of alkaline "alperujo" compost. Bioresour. Technol. 102, 1481–1488.

Giro, M.E.A., Garcia Jr., O., Zaiat, M., 2006. Immobilized cells of *Acidithiobacillus ferrooxidans* in PVC strands and sulfite removal in a pilot-scale bioreactor. Chem. Eng. J. 28, 201–207.

Gomez, J., Cantero, D., Webb, C., 2000. Immobilisation of *Thiobacillus ferrooxidans* cells on nickel alloy fibre for ferrous sulfate oxidation. Appl. Microbiol. Biotechnol. 54, 335–340.

Goncalves, J.J., Govind, R., 2009. Enhanced biofiltration using cell attachment promotors. Environ. Sci. Technol. 43, 1049–1054.

González-Sánchez, A., Revah, S., Deshusses, M.A., 2008. Alkaline biofiltration of H_2S odors. Environ. Sci. Technol. 42, 7398–7404.

Ho, K.L., Chung, Y.C., Lin, Y.H., Tseng, C.P., 2008. Microbial populations analysis and field application of biofilter for the removal of volatile-sulfur compounds from swine wastewater treatment system. J. Hazard. Mater. 152, 580–588.

Jiang, X., Yan, R., Tay, J.H., 2009. Simultaneous autotrophic biodegradation of H_2S and NH_3 in a biotrickling filter. Chemosphere 75, 1350–1355.

Johnson, D.B., Okibe, N., Hallberg, K.B., 2005. Differentiation and identification of iron-oxidizing acidophilic bacteria using cultivation techniques and amplified ribosomal DNA restriction enzyme analysis. J. Microbiol. Methods 60, 299–313.

Khalid, A., Bhatti, T., Umar, M., 1993. An improved solid medium for isolation, enumeration and genetic investigations of autotrophic iron-and sulphur-oxidizing bacteria. Appl. Microbiol. Biotechnol. 39, 259–263.

Kim, J.H., Rene, E.R., Park, H.S., 2008. Biological oxidation of hydrogen sulfide under steady and transient state conditions in an immobilized cell biofilter. Bioresour. Technol. 99, 583–588.

Kim, T.W., Kim, C.J., Chang, Y.K., Ryu, H.W., Cho, K.S., 2002. Development of an optimal medium for continuous ferrous iron oxidation by immobilized *Acidothiobacillus ferrooxidans* cells. Biotechnol. Prog. 18, 752–759.

Lee, E.Y., Lee, N.Y., Cho, K.-S., Ryu, H.W., 2006. Removal of hydrogen sulfide by sulfate-resistant *Acidithiobacillus thiooxidans* AZ11. J. Biosci. Bioeng. 101, 309–314.

Mesa, M., Andrades, J., Macias, M., Cantero, D., 2004. Biological oxidation of ferrous iron: study of bioreactor efficiency. J. Chem. Technol. Biotechnol. 79, 163–170.

Mousavi, S.M., Yaghmaei, S., Vossoughi, M., Roostaazad, R., Jafari, A., Ebrahimi, M., Chabok, O.H., Turunen, I., 2008. The effects of Fe(II) and Fe(III) concentration and initial pH on microbial leaching of low-grade sphalerite ore in a column reactor. Bioresour. Technol. 99, 2840–2845.

Pagella, C., De Faveri, D., 2000. H_2S gas treatment by iron bioprocess. Chem. Eng. Sci. 55, 2185–2194.

Ramírez, M., Fernández, M., Granada, C., Le Borgne, S., Gómez, J.M., Cantero, D., 2011. Biofiltration of reduced sulphur compounds and community analysis of sulphur-oxidizing bacteria. Bioresour. Technol. 102, 4047–4053.

Ryu, H.W., Yoo, S.-K., Choi, J.M., Cho, K.-S., Cha, D.K., 2009. Thermophilic biofiltration of H_2S and isolation of a thermophilic and heterotrophic H_2S-degrading bacterium, *Bacillus* sp. TSO3. J. Hazard. Mater. 168, 501–506.

Torsvik, V., Øvreås, L., Nakatsu, C.H., 2000. Soil community analysis using DGGE of 16S rDNA polymerase chain reaction products. Soil Sci. Soc. Am. J. 64, 1382–1388.